Description of relativistic heavy-light quark-antiquark systems via Dirac equation

V. D. Mur, V. S. Popov, Yu. A. Simonov, and V. P. Yurov

Institute of Theoretial and Experimental Physics, 117259 Moscow, Russia
(Submitted 25 June 1993)
Zh. Eksp. Teor. Fiz. **105**, 3–27 (January 1994)

Starting from the QCD Lagrangian and taking into account both perturbative and nonperturbative effects, we use the method of vacuum correlators to derive the Dirac equation (rigorously for the Coulomb interaction and heuristically for the confining potential) for a system consisting of a light quark and heavy antiquark. As a result the confining potential is a Lorentz scalar, and the Coulomb part the fourth component of a 4-vector. The energy spectrum of the Dirac equation is considered for these potentials. Numerical calculations of energy eigenvalues $E=E_{n\kappa}$ are performed, and some exact solutions of the Dirac equation in the case $E=0$ are found. An effective-potential method convenient for qualitative study of the solutions of the Dirac equation is developed. The connection with experimental spectra of D- and B-mesons is briefly discussed.

1. INTRODUCTION

The quark-antiquark systems consisting of one heavy quark (antiquark) Q and one light antiquark (quark) $\bar{q}$ are QCD analogs of the hydrogen atom and thus are of fundamental importance.

Recently the issue of the heavy-light bosons has become a topic of vivid interest in both analytic and Monte Carlo QCD studies.[1]

From the theoretical viewpoint the interest in heavy-light systems stems from several considerations. First, in the limit of one infinitely heavy quark, one hopes to get the dynamics of a light quark in the external field of a heavy one. That would be similar to the picture of the hydrogen atom.

Second, since the external field is time-independent, one may hope to obtain a static potential in QCD together with spin-dependent forces, as has been done for heavy quarkonia.[2]

An important issue in this connection is the Lorentz nature of the confining part of the potential. Arguments in favor of a scalar nature are found in the form of inequalities[3] and also in the form of spin-dependent terms.[2,4]

Third, in the heavy-light system one may study how the chiral symmetry breaking (CSB) affects the spectrum. When one quark mass is vanishing, in the chiral symmetric case the spectrum would consist of parity doublets, and the CSB would lift the degeneracy.

Fourth, using the Dirac equation we implement explicitly relativistic dynamics and can study relativistic properties of the spectrum, e.g., in the case of a vanishing quark mass, and also relativistic spin splittings in the spectrum.

In particular, in our case the spin symmetry now being widely discussed[1] is present, since the spin of the heavy quark is decoupled. Hence every state of the Dirac equation with a given j and parity corresponds to two almost degenerate states of the $(q\bar{Q})$ system with j and the heavy quark spin $S=1/2$ adding to $J=j\pm 1/2$.

Our final point is that the Dirac equation description yields a dynamical framework for the heavy-light mesons which can be used to calculate meson matrix elements and form factors to compare with experiment and semiphenomenological approaches now widely used in this context.[1,5]

Here we attempt to derive explicitly the Dirac equation for the heavy-light quark system starting from the QCD Lagrangian and incorporating both perturbative and nonperturbative effects in the framework of the vacuum correlator method (VCM).[6–8]

In the course of the derivation we use some approximations, which are clearly stated at each step, e.g., neglect of virtual quark pairs (the quenching approximation), keeping the lowest (quadratic) cumulant in the cluster expansion, and the "limit of local dynamics,"[2] $T_g\to 0$, where T_g is the gluonic vacuum correlation length. We discuss physical implications of these approximations in the main text below.

Even with those approximations we are unable to prove rigorously the appearance of a static scalar confining potential, but we give strong arguments in favor of it. The situation is much better for the perturbative part, and the existence of an external vector potential in the limit of one heavy quark mass is explicitly shown.

At this point we start with the Dirac equation containing a vector Coulomb part and a scalar confining part, and we study properties of its spectrum. For comparison we also consider two other cases: i) the equation has a vector confining part and a Coulomb part; ii) both parts of the potential transform as scalars. We are explicitly interested in the limit of a vanishing light quark mass and the spin dependence of the energy eigenvalues.

We show explicitly that a reasonable spectrum occurs only for a scalar confining part. In this case the scalar potential breaks explicitly chiral symmetry, and states with opposite parities are not degenerate. In the case of a vector confining part, only quasistationary states are found.

We write possible general symmetry properties of spectral states and also the corresponding properties in the

 1063-7761/94/010001-14$10.00

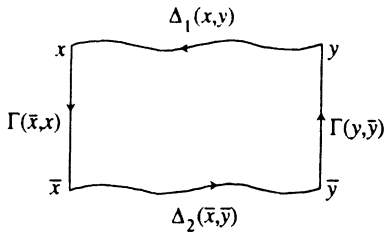

FIG. 1. Quark-antiquark Green's function describing transition from the initial state $\Gamma(y,\bar{y})$ to the final state $\Gamma(x,\bar{x})$. Wavy lines refer to the quark (antiquark) Green's function $\Delta_1(x,y)$ $[\Delta_2(x,y)]$.

particular cases of a zero scalar potential, a zero vector potential, and a zero mass.

We also find some exact analytic solutions of the Dirac equation which occur for $E=0$. This enables us to find an equation, which determines that value of the Coulomb constant ($\zeta=\zeta_{nx}$), for which the (njl) discrete energy level reaches the value $E=0$. We note an analogy of this problem with the relativistic Coulomb problem of an electron in the field of a heavy supercritical nucleus with $Z>137$.[9-11]

The paper is organized as follow. In Sec. 2 we use the Feynman-Schwinger representation of the quark-antiquark Green function to derive the limit of one infinite mass.

In Sec. 3 we compare this limit with the Dirac equation and discuss the Lorentz nature of the confining interaction.

In Sec. 4 we discuss the properties of the spectrum of the Dirac equation.

In Sec. 5 we discuss symmetry properties of the spectrum, in particular chiral properties.

In Sec. 6 we discuss numerical results for the spectrum of the Dirac equation in the limit of a vanishing small quark mass.

In Sec. 7 we investigate the exact analytic solutions of the Dirac equation which occur for $E=0$.

In Sec. 8 we summarize our results and compare the Dirac spectrum obtained here with experiment and other approaches. This enables us to also discuss large-mass corrections.

2. FEYNMAN–SCHWINGER REPRESENTATION FOR THE HEAVY-LIGHT GREEN'S FUNCTION

Consider the quark-antiquark system of one heavy antiquark (with mass m_2) and a light quark of much smaller mass m_1, which we neglect in some cases below.

The Green's function G of such a system, with the quarks initially at points $y,\bar{y}$ and finally at points $x,\bar{x}$, is given by the path integral over fermionic and gluonic fields A in Ref. 8. Evaluating the fermionic integrals and neglecting the fermionic determinants (the quenching approximation) for simplicity, one arrives at the amplitude depicted graphically in Fig. 1, where Δ_i is the quark Green's function with quark mass m_i, and the Γ's belong to the initial and final wave functions:

$$\Psi(y,\bar{y})=\bar{q}(y)\Gamma(y,\bar{y})q(\bar{y}),$$

with a similar expression for $\Psi(x,\bar{x})$. Thus we can write

$$G(x\bar{x}|y\bar{y})=\langle \mathrm{tr}[\Gamma(\bar{x},x)\Delta_1(x,y)\Gamma(y,\bar{y})\Delta_2(\bar{y},\bar{x})]\rangle. \quad (1)$$

The angular brackets here denote the integration over gluonic fields. This integration we perform using the cluster expansion.[6,7] We arrive at the following expression involving proper-time and path integrals for the quark (s,z) and the antiquark $(\bar{s},\bar{z})$:

$$G(x\bar{x}|y\bar{y})=\int_0^\infty ds\int_0^\infty d\bar{s}DzD\bar{z}e^{-K-\bar{K}}\mathrm{tr}[\Gamma_x(m_1-\hat{D}^{(1)})\gamma_{z\bar{z}}\Gamma_y(m_2-\hat{D}^{(2)})], \quad (2)$$

where

$$K=m_1^2s+\frac{1}{4}\int_0^s \dot{z}^2d\tau,$$

$$\bar{K}=m_2^2\bar{s}+\frac{1}{4}\int_0^{\bar{s}}\dot{\bar{z}}^2d\bar{\tau}.$$

In (2), Γ_x, Γ_y refer to the Lorentz structures in the initial and final states, and $D^{(i)}$ and $\gamma_{z\bar{z}}$ are given in Ref. 7. We rewrite the latter here in the following form (in the lowest order of a cluster expansion, where perturbative and nonperturbative contributions factorize[8]):

$$\gamma_{z\bar{z}}=\exp\left[-\frac{g^2}{2}\int df_{\mu\nu}(u)df_{\rho\lambda}(u')\times\langle F_{\mu\nu}(u)F_{\rho\lambda}(u')\rangle\right], \quad (3)$$

where

$$df_{\mu\nu}(u)\equiv ds_{\mu\nu}(u)-i\sigma^{(1)}_{\mu\nu}d\tau+i\sigma^{(2)}_{\mu\nu}d\bar{\tau}, \quad (4)$$

and $\langle F\,F\rangle$ is the gluonic correlator. The latter can be split into perturbative and nonperturbative parts as in Ref. 7.

Now we discuss the limit of one heavy mass, $m_2\to\infty$. In this case, when m_2 is much larger than the interaction strength, particle 2 is moving along the straight-line trajectory

$$\bar{z}_\mu=\bar{y}_\mu+\frac{\bar{x}_\mu-\bar{y}_\mu}{\bar{s}}\tau,\quad 0\leqslant\bar{\tau}\leqslant\bar{s},$$

$$\bar{x}_4-\bar{y}_4\equiv T,\quad \frac{T}{\bar{s}}=2m_2,\quad d\bar{\tau}=\frac{d\bar{z}_4}{2m_2}; \quad (5)$$

$\bar{x}_i=\bar{y}_i=R_i$ is the position in space of particle 2.

One can see that in this limit the spin interaction of particle 2 (terms $\sigma^{(2)}d\bar{\tau}$) is $\sim O(1/m_2)$ and can be neglected.

The perturbative part of the cumulant $\langle\langle F(x)F(y)\rangle\rangle$ can be written as[6,7]

$$g^2\int d\sigma_{\mu\nu}(u)\int d\sigma_{\rho\lambda}(u')\langle\langle F_{\mu\nu}(u)F_{\rho\lambda}(u')\rangle\rangle_{\mathrm{pert}}$$

$$=g^2\int_C dz_\mu\int_C dz'_\rho\langle A_\mu(z)A_\rho(z')\rangle_{\mathrm{pert}}$$

$$=\frac{C_2 g^2}{4\pi^2}\int_C dz_\mu \int_C \frac{dz'_\mu}{(z-z')^2}, \qquad (6)$$

where C_2 is the quadratic Casimir operator, $C_2(N_C=3)=4/3$, and C is the closed contour depicted in Fig. 1. The integral in (6) is divergent and is regularized by inserting a Z factor in front of the exponential in (3) and introducing the minimal distance δ of the points $\bar{z}$ and $\bar{z}'$ in (6) (for details see Ref. 12).

Therefore we can now study the situation when only the perturbative interaction is present, and the Green's function looks like

$$\begin{aligned} G(x\bar{x}|y\bar{y}) = \int_0^\infty ds Dz \exp\left(-m_1^2 s - \frac{1}{4}\int_0^s \dot{z}^2 d\tau\right) \\ \times \mathrm{tr}\left[\Gamma_x\left(m_1+\frac{1}{2}\dot{z}\right)Z\right. \\ \times \exp\left[-g^2\int\left(ds_{\mu\nu}(u)+\frac{1}{i}\sigma^{(1)}_{\mu\nu}d\tau\right)\right. \\ \left.\left.\times ds_{\rho\lambda}(u')\langle\langle F_{\mu\nu}(u)F_{\rho\lambda}(u')\rangle\rangle_{\mathrm{pert}}\right]\right. \\ \left.\times\Gamma_y(m_2(1-\gamma_4))\right], \qquad (7) \end{aligned}$$

where we have neglected terms representing the self-interaction of particle 1.

Our goal now is to rewrite the exponential function in (7) in the form

$$\exp\left[ig\int\left(\bar{A}_\mu(z)dz_\mu+\frac{1}{i}\sigma^{(1)}_{\mu\nu}\bar{F}_{\mu\nu}d\tau\right)\right] \qquad (8)$$

(a similar derivation for QED was done in Ref. 13), where we have defined (following Ref. 6)

$$\begin{aligned} \bar{A}_\mu(z) &= ig\int\langle A_\mu(z)A_\rho(z')\rangle dz'_\rho \\ &= \frac{ig}{4\pi^2}\int\frac{dz'_\mu}{(z-z')^2} \\ &= \frac{ig}{4\pi}\frac{\delta_{\mu 4}}{|z-\mathbf{R}|}C_2. \end{aligned} \qquad (9)$$

Similarly,

$$\bar{F}_{\mu\nu}=\partial_\mu\bar{A}_\nu-\partial_\nu\bar{A}_\mu. \qquad (10)$$

One can also verify that the explicit expression for $\langle\langle F F\rangle\rangle_{\mathrm{pert}}$, which one obtains from the Feynman gauge propagator,[6] leads to

$$\langle A_\mu(z)A_\nu(z')\rangle_{\mathrm{pert}}=\frac{1}{4\pi^2}\frac{\delta_{\mu\nu}}{(z-z')^2}. \qquad (11)$$

Hence we can write the $q\bar{q}$ Green's function, keeping only the perturbative interaction:

$$G(x\bar{x}|y\bar{y})=\mathrm{tr}[\Gamma_x G(x,y)\Gamma_y m_2(1-\gamma_4)], \qquad (12)$$

where we have defined

$$\begin{aligned} G(x,y) &= \int ds Dz[m_1-\hat{D}(\bar{A})]\exp\left(-m_1^2 s-\frac{1}{4}\int_0^s\dot{z}^2 d\tau\right. \\ &\quad \left.+ig\int_y^x\bar{A}_\mu dz_\mu+g\int_0^s\sigma_{\mu\nu}\bar{F}_{\mu\nu}d\tau\right) \\ &= \left\langle x\left|\int_0^\infty ds[m_1-\hat{D}(\bar{A})]\exp\{-s[m^2\right.\right. \\ &\quad \left.\left.-\hat{D}^2(\bar{A})]\}\right|y\right\rangle \\ &= \langle x|[m_1+\hat{D}(\bar{A})]^{-1}|y\rangle. \end{aligned} \qquad (13)$$

We observe that $G(x,y)$ satisfies the Dirac equation

$$[m_1+\hat{D}(\bar{A})]G(x,y)=\delta^{(4)}(x-y). \qquad (14)$$

In the next section we study the effect of the nonperturbative interaction.

3. CONFINING FORCE AND THE DIRAC EQUATION

We now turn to the nonperturbative interaction, which provides confinement due to the presence of the special (Kronecker) structure in the quadratic cumulant.[6] Again neglecting the self-interaction of light particle, we find an equation of the same form as (7), but we should add $\langle\langle F F\rangle\rangle_{\mathrm{pert}}$ also the nonperturbative part $\langle\langle FF\rangle\rangle_{\mathrm{nonpert}}$, which can be written as[6]

$$\begin{aligned} \langle\langle F_{\mu\nu}(u)F_{\rho\lambda}(u')\rangle\rangle &= (\delta_{\mu\rho}\delta_{\nu\lambda}-\delta_{\mu\lambda}\delta_{\nu\rho})D(u-u') \\ &\quad +\frac{1}{2}\left\{\frac{\partial}{\partial u_\mu}[(u-u')_\rho\delta_{\nu\lambda}-(u\right. \\ &\quad \left.-u')_\lambda\delta_{\nu\rho}]+\mu\rho\leftrightarrow\nu\lambda\right\} \\ &\quad \times D_1(u-u'). \end{aligned} \qquad (15)$$

It has been shown[6,7] that only D (and not D_1) yields confinement (the area law of the Wilson loop). We concentrate first on this term, disregarding also the spin term $\sigma^{(1)}_{\mu\nu}$ in (7). We have

$$\begin{aligned} &\int ds_{\mu\nu}(u)\int ds_{\rho\lambda}(u')\langle\langle F_{\mu\nu}(u)F_{\rho\lambda}(u')\rangle\rangle \\ &\quad\to\int ds_{\mu\nu}(u)ds_{\mu\nu}(u')D(u-u')+\dots. \end{aligned} \qquad (16)$$

Using the same arguments as in Ref. 6, one can see that we get the area-law exponential function in Ref. (7). Namely, for large area we have

$$\exp(-\sigma S_{\min}),\quad \sigma=\frac{1}{2}\int\int d^2u D(u), \qquad (17)$$

where $S_{\min}$ is the minimal area inside the contour formed by the straight-line trajectory of the heavy particle and the path $z(\tau)$ of the light one.

We are now facing some fundamental questions: i) Can the term (17) be associated with a local potential V,

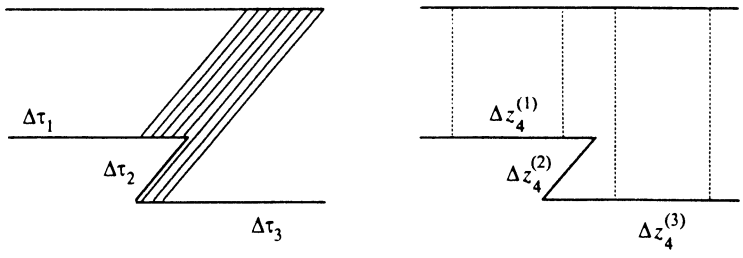

FIG. 2. Trajectory corresponding to virtual pair creation. a—Scalar case; b—vector case.

acting on particle 1? ii) What are the Lorentz properties of this potential—does it transform as a scalar or as a vector?

To answer question i) we follow the arguments given in Ref. 2. We must therefore return to the exponential function in (3), defining the dynamics of the system. The integral in the exponential function in (3) is over the surface inside the quark and antiquark trajectories; the characteristic length of these trajectories is T_q, a period of quark orbiting.

Being at some point $z(\tau_0)$ on the trajectory, a quark is influenced by the fields and through them by its partner. The radius of nonlocality of the fields is given by the correlation length T_g, defining behavior of $\langle F(u)F(u')\rangle$, i.e., by the functions $D[(u-u')/T_g]$, $D_1[(u-u')/T_g]$.

Therefore the criterion of local dynamics is $T_q \gg T_g$.[2,14]

In the opposite case, $T_q \leqslant T_g$, the quark "feels" all the fields and also the motion of the antiquark during all its history. This is the nonlocal dynamics, which can be treated by the QCD sum rules.[15] Lattice calculations yield $T_g \sim 0.2$–0.3 fm,[16] while T_q for both the light and heavy quarks is $T_q \geqslant 1$ fm. Therefore the actual situation is close to the local dynamics.

Regarding the first point, we proceed as in Refs. 8, 17, forming the minimal surface via the connection of $\gamma \equiv \bar{\tau}/\bar{s} = \tau/s = t/T$, where $t = \bar{z}_4 - \bar{y}_4$.

In this case, combining all exponential functions in (13) and (17), we obtain

$$B = \int_0^T dt \left[\frac{m_1^2}{2\mu_1} + \frac{\mu_1}{2} + \frac{\mu_1}{2} \dot{r}_\alpha^2(t) + \sigma \int_0^1 d\beta \sqrt{\dot{w}^2 r^2 - (\dot{w}_\mu r_\mu)^2} \right], \tag{18}$$

where we have defined, as in Refs. 8, 18,

$$w_\mu(t) = z_\mu(t)\beta + \bar{z}_\mu(t)(1-\beta), \quad \dot{w}_\mu = \frac{\partial}{\partial t} w_\mu,$$

$$r_\mu(t) = z_\mu(t) - \bar{z}_\mu(t), \quad 2\mu_1 = T/s. \tag{19}$$

Taking (5) into account, we have

$$w_i(t) = z_i(t)\beta + R_i(1-\beta), \quad R_i = \text{const},$$

$$w_4(t) = z_4(t)\beta + (\bar{y}_4 + t)(1-\beta),$$

$$\dot{w}_i(t) = \dot{z}_i(t)\beta = \dot{r}_i(t)\beta, \quad \dot{w}_4 = \dot{z}_4(t)\beta + 1 - \beta. \tag{20}$$

Following the same procedure as in Refs. 8, 18, we obtain from B (considered as an action) the proper-time Hamiltonian, which depends on the dynamical mass μ_1:

$$H(\mu_1) = \frac{m_1^2}{2\mu_1} + \frac{\mu_1}{2} + \sigma|\mathbf{r}| + \frac{1}{2\mu_1}\left(-\frac{\partial^2}{\partial \mathbf{r}^2}\right). \tag{21}$$

The eigenvalue of $H(\mu_1)$ is to be minimized with respect to μ_1; the final value of μ_1 is determined in this manner.

Thus we see that the nonperturbative correlator $\langle\langle FF\rangle\rangle_{\text{nonpert}}$ does indeed yield a potential-type term in the proper-time Hamiltonian, provided T_g is small[2] and the expansion of the square-root term in β is done as in Ref. 18 (the corresponding error is $\sim 10\%$).

It is more difficult to answer the other question—about the Lorentz nature of this potential—since Eq. (21) is written in the c.m. system, and we do not know how this expression transforms under Lorentz boosts. To get a partial understanding of this point, let us compare how the vector and scalar potentials enter the Feynman-Schwinger representation for the Green's function of a scalar quark [i.e., neglecting a spin term $\sim\sigma^{(1)}$ in (13)].

For the scalar case we can write

$$G(x,y) \sim \int ds Dz \exp\left[-\int_0^s V_s(z(\tau))d\tau - m^2 s - \int_0^s \frac{\dot{z}^2}{4} d\tau \right], \tag{22}$$

while for the vector case we have

$$G(x,y) \sim \int ds Dz \exp\left(-m^2 s - \int_0^s \frac{\dot{z}^2}{4} d\tau + i \int s_0 V_\mu dz_\mu \right). \tag{23}$$

The main difference lies in the fact that trajectories of the Z-type depicted in Fig. 2 (virtual pair creation) give different contributions in the scalar and vector case. For the scalar case the proper time intervals $\Delta\tau_1$, $\Delta\tau_2$, and $\Delta\tau_3$ are positive and add together, thereby suppressing the pair creation, while in the vector case $\Delta z_4^{(1)}$, $\Delta z_4^{(2)}$, and $\Delta z_4^{(3)}$ strongly cancel each other, making pair creation easy. In other words, for the scalar potential all parts of a trajectory

add arithmetically, while for the vector potential should take a vector sum of all intervals along the trajectory.

Looking at our prototype of the potential, the last term in (18), one can see that in this case one actually adds a scalar quantity $\dot{\sigma}dt\sqrt{\ }$ (we recall that dt is not the fourth component of a vector, but rather the proper time $d\tau$, which is scalar). Thus we seem to be justified in treating the confining force as a scalar and not a vector.

There are additional arguments in favor of this conclusion.

First of all, in the nonrelativistic derivation of spin-dependent forces in nonperturbative QCD,[2] the sign and magnitude of the spin-orbit term depend on whether the confining potential is chosen as a scalar or a vector.[4] In Appendix B we reproduce the spin-dependent terms obtained in Ref. 2, for the case of two nonrelativistic quarks. One can notice that the asymptotically dominant contribution comes from V_1', which contains only a scalar contribution and yields the negative coefficient of the spin-orbit term LS, characteristic of Thomas precession.

Results obtained in Ref. 2 through the use of the cluster expansion and the area law unambigiously predict the spin-orbit force corresponding to the Thomas precession term, which was also introduce a previously using the string picture.[19] All that corresponds to scalar confinement.

Second, there are independent arguments in Ref. 3 which lead to inequalities which are satisfied for the scalar confining potential, and not satisfied for the vector case. Finally, the vector confining potential is believed to cause the Klein paradox.[10,11] In Secs. 4 and 6 we study both scalar and vector confining potentials and show analytically and numerically that, indeed, only in the first case does one obtain a physically consistent spectrum, corresponding to confinement while in the second case one has only quasistationary states. This situation is related to the Klein paradox.[10,11] Thus we give strong arguments in favor of the scalar confining potential. Unfortunately at the moment we are still unable to derive from the Feynman–Schwinger representation the Dirac equation with the scalar potential, in the way we have done for a perturbative Coulomb interaction.

Therefore in the next sections we simply postulate the Dirac equation with a confining potential of the scalar type (or vector type—to check its inconsistency).

4. PROPERTIES OF THE SPECTRUM OF THE DIRAC EQUATION

As we showed in the previous sections, the color Coulomb interaction between quarks is of a vector nature. We have argued that the confining interaction is a scalar. It is instructive, nevertheless, to consider both possibilities for the interactions, scalar U and vector V, and to study the properties of solutions of the Dirac equation in these cases.

Assuming spherical symmetry, we look for solutions of the Dirac equation in the form

$$\Psi=r^{-1}\begin{pmatrix} G(r)\Omega_{jl_M} \\ iF(r)\Omega_{jl'_M}\end{pmatrix}, \tag{24}$$

where $l+l'=2j$, and the Ω's are spherical spinors.[20]

Equations for radial wave functions are

$$\frac{dG}{dr}+\frac{\kappa}{r}G-[E+m+U(r)-V(r)]F=0,$$

$$\frac{dF}{dr}-\frac{\kappa}{r}F+[E-m-U(r)-V(r)]G=0, \tag{25}$$

where E and m are the energy and mass of the light particle ($m\equiv m_1$ in the notation of Sec. 2), and

$$\kappa=\begin{cases} -(l+1), & \text{if } j=l+1/2, \\ l, & \text{if } j=l-1/2, \end{cases} \tag{26}$$

so that $|\kappa|=j+1/2=1,2,\ldots$. We consider three choices.

a) Assume

$$U(r)=M^2r, \quad V(r)=-\frac{\zeta}{r}, \quad M^2\equiv\sigma; \quad \zeta=\frac{4}{3}\alpha_s. \tag{27}$$

Putting $m=0$ and introducing the dimensionless variables $x\equiv Mr$ and $\varepsilon=E/M$, we arrive at

$$G'+\frac{\kappa}{x}G-\left(\varepsilon+x+\frac{\zeta}{x}\right)F=0,$$

$$F'-\frac{\kappa}{x}F+\left(\varepsilon-x+\frac{\zeta}{x}\right)G=0 \tag{28}$$

(hereafter the prime denotes the derivative with respect to x).

Let us find the asymptotics of the radial functions at zero and infinity. For $x\to 0$, inserting the expansions

$$G=Ax^{\nu}+\ldots, \quad F=Bx^{\nu}+\ldots$$

into (28), we obtain

$$\nu=(\kappa^2-\zeta^2)^{1/2}, \quad A/B=\kappa^{-1}(\kappa^2-\zeta^2)^{1/2}-1. \tag{29}$$

The wave function is regular at zero for $\zeta<|\kappa|=j+1/2$ while for $\zeta>j+1/2$ there occurs a "collapse to the center" (well known in quantum mechanics).[21,22] The difficulty is actually of a formal character and can be removed by introducing a cutoff of the Coulomb potential at small distances, $r<r_0$—in the same way as in QED with the charge $Z>\alpha^{-1}=137$ (see Refs. 9–11, 23, 24).

The behavior of the wave functions at infinity is more complicated. From (28) it follows that $G,F\sim\exp(\pm x^2/2)$ as $x\to\infty$, and the solution with a positive exponent is clearly not admissible.

We accordingly write G,F as

$$G\approx A'\exp[-(ax^2+bx)]x^{\beta}\left(1-\frac{c_1}{x}+\frac{c_2}{x^2}+\ldots\right),$$

$$F\approx B'\exp[-(ax^2+bx)]x^{\beta}\left(1-\frac{c_1'}{x}+\frac{c_2'}{x^2}+\ldots\right). \tag{30}$$

Inserting these expansions into (28) we find, after some elementary but cumbersome calculations,

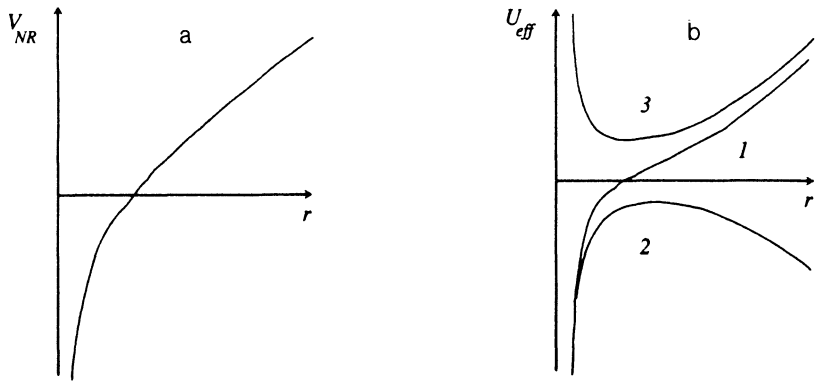

FIG. 3. Nonrelativistic potential $V_{NR}(r)$ (a) and effective potential $U_{\text{eff}}(r)$ (b) for various Lorentz structures of the interaction. Curves *1–3* correspond to the three choices in Sec. 4.

$$A'=-B',\quad a=1/2,\quad b=0,\quad \beta=\varepsilon^2/2,$$

$$c_1=(\zeta-1/2)\varepsilon,\quad c_1'=(\zeta+1/2)\varepsilon,\ldots. \tag{31}$$

The following coefficients, $c_2,c_2',\ldots$, can be calculated by means of recurrence relations[1)].

Thus the wave functions fall off at infinity mostly in the same way as in the case of the harmonic oscillator in nonrelativistic quantum mechanics. The solution satisfying the conditions obtained above, (29) and (30), exists only for certain values of $\varepsilon=\varepsilon_n(\zeta,\kappa)$, and the wave function is normalizable. Therefore, for the Dirac equation only a discrete spectrum exists.

This conclusion holds for any scalar potential which grows at infinity,

$$G(r),F(r)\sim\exp\left[-\int_0^r U(r)dr'\right],\quad r\to\infty. \tag{32}$$

Even for the logarithmic potential the wave functions decrease asymptotically faster than exponentially:

$$G,F_{(r\to\infty)}\sim\exp(-gr\ln r)\quad\text{for}\quad U(r)=g\ln r.$$

b) When both interactions are of a vector type, i.e.,

$$U(r)=0,\quad V(r)=-\zeta r^{-1}+M^2r, \tag{33}$$

the system of radial equations is

$$G'+\frac{\kappa}{x}G-\left(\varepsilon+\frac{\zeta}{x}-x\right)F=0,$$

$$F'-\frac{\kappa}{x}F+\left(\varepsilon+\frac{\zeta}{x}-x\right)G=0. \tag{34}$$

In this case, at $x\to0$ we have

$$\nu=(\kappa^2-\zeta^2)^{1/2},\quad A/B=\kappa/[\kappa+(\kappa^2-\zeta^2)^{1/2}],$$

while the parameters in Eq. (30) assume the values

$$A'=iB',\quad a=-i/2,\quad b=i\varepsilon,\quad \beta=-i\zeta.$$

Here we chose a solution satisfying the Sommerfeld radiation condition, i.e., having an outgoing wave at $r\to\infty$. Thus for interaction (33) the discrete spectrum is absent (see also curve *2* in Fig. 3), and all solutions of the Dirac equation, if any, are quasistationary. In the special case of a square well one can obtain an exact analytic equation for the spectrum.[25] The width of these quasistationary states determines the probability of spontaneous pair creation in potential (33). This phenomenon is closely connected with the Klein paradox.[10,11] Physically it means that the problem is now of the many-particle type, but actually the Dirac equation is still applicable.

c) For completeness, consider also the case of purely scalar interactions,

$$U=-\zeta r^{-1}+M^2r,\quad V=0. \tag{35}$$

In this case we have at $r\to0$, instead of (29),

$$\nu=(\kappa^2+\zeta^2)^{1/2},\quad A/B=[\kappa-(\kappa^2+\zeta^2)^{1/2}]/\zeta. \tag{36}$$

Thus the "collapse to the center" does not occur for arbitrary large values of the Coulomb parameter ζ. At infinity we obtain a behavior which is analogous to (30):

$$G,F\sim\exp(-M^2r^2/2);$$

therefore the spectrum is discrete.

Hence the character of the energy spectrum depends crucially on the assumption about the nature of the confining interaction M^2r (scalar or vector).

The reason can be understood qualitatively by using the method of an effective potential.[24,26]

System (25) corresponds in the quasiclassical approximation (neglecting spin-orbit and spin-spin forces) to the following relation between energy and momentum

$$p^2(r)=[E-V(r)]^2-[m+U(r)]^2+\kappa^2r^{-2}$$
$$\equiv2m(\tilde{E}-U_{\text{eff}}), \tag{37}$$

where $\tilde{E}$ and U_{eff} are the effective energy and potential in the nonrelativistic Schrödinger equation:

$$\tilde{E}=\frac{1}{2m}(E^2-m^2),\quad U_{\text{eff}}=\frac{1}{2m}(U^2-V^2)+U+\frac{\kappa^2}{2mr^2}. \tag{38}$$

In the nonrelativistic limit ($E\approx m$ and $U,|V|\ll m$) we have

$$U_{\text{eff}}\approx U+V+(l+1/2)^2/2mr^2.$$

Therefore, all three cases, a)–c) correspond to the tunnel potential

$$U_{\text{eff}}(r)=-\zeta/r+\sigma r,$$

which is often used in QCD.

However, for large U and V, the situation is drastically different for our cases a)–c). This can be understood from Fig. 3, where the qualitative behavior of $U_{\text{eff}}(r)$ is shown. Using the effective-potential method, one can also perform a quantitative study of the problem (for details see Appendix A). Applying the WKB method and taking into account Eq. (37), one can easily determine the asymptotics of the wave functions at infinity.

For example, in case a) we get

$$G,F\sim\exp\left(-\int_0^x |p|dx\right),$$

$$|p|=U+m-\frac{\varepsilon^2}{2U}+\frac{\varepsilon V}{U}+\dots . \tag{39}$$

If $U(x)=gx^\alpha,\alpha>0$, and $V(x)=-\zeta/x$, then at $x\to\infty$ we find

$$G\approx -F$$

$$\sim\begin{cases}\exp\{-[gx^2/2+mx-(2g)^{-1}\varepsilon^2\ln x]\}, & \alpha=1,\\ \exp\{-[g(\alpha+1)^{-1}x^{\alpha+1}+mx]\}, & \alpha>1.\end{cases} \tag{40}$$

The first formula (with $g=1$ and $m=0$) explains the structure of asymptotic expansion (30).

5. SYMMETRY PROPERTIES OF THE SPECTRUM OF THE DIRAC EQUATION

Here we discuss symmetries of solutions of the Dirac equation for particles of zero mass.

It is clear that when both m and U are zero the Dirac equation (and the corresponding term in the Lagrangian) is chirally symmetric, i.e., does not change under a global transformation:

$$\Psi\to\exp(i\alpha\gamma_5)\Psi,\quad \bar\Psi\to\bar\Psi\exp(i\alpha\gamma_5). \tag{41}$$

From the point of view of the spectrum the chiral symetry means that all states are parity degenerate; i.e., the masses of the states 0^+ and 0^- (or 1^+ and 1^-) are the same.

It is easy to demonstrate that system (25) with $m=0$ is invariant under even more general transformations when $U\neq 0$:

$$E\to E,\quad \kappa\to-\kappa,\quad U\to -U,\quad V\to V,$$

$$G(r)\to -F(r),\quad F(r)\to G(r). \tag{42}$$

It follows from (42) that for $U\equiv 0$ the spectrum is degenerate with respect to the sign of the Dirac quantum number κ; i.e., it depends on only the total momentum j, not on the way l and s are coupled (chiral degeneracy).

Another symmetry of the Dirac equation is

$$E\to -E,\quad \kappa\to-\kappa,\quad U\to U,$$

$$V\to -V,\quad G(r)\leftrightarrow F(r), \tag{43}$$

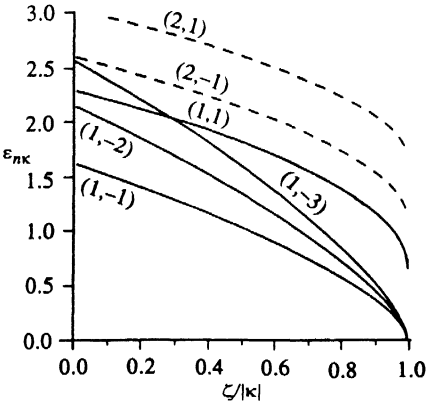

FIG. 4. Energy spectrum for the Dirac equation with potential (27). The solid curves correspond to the $n=1$ states, the dashed ones to $n=2$. The curves are labeled with the values of κ.

which in contrast to (42) connects states with positive and negative energy. In particular, for $V\equiv 0$ (scalar interaction) there is a doubling of states with a given $|E_n|,E_n=\pm|E_n|$, and we can always consider $E_n>0$. In the specific case $E=0$ (zero modes) there is, at first sight, a chiral degeneracy of states. However, it is easy to show that the degenerate states with $E=0$ do not exist at all. Multiplying the first equation in (25) by G, multiplying the second by F, and integrating the difference from $r=0$ to $r=\infty$, we obtain an identity:

$$\int_0^\infty (G^2+F^2)\frac{dr}{r}=2\kappa^{-1}\int_0^\infty (E-V)GFdr \tag{44}$$

(we have used in the derivation the circumstanse that G and F vanish at both $r=0$ and $r=\infty$). From Eq. (44) one can see that for the purely scalar interaction there are no solutions with zero energy.

Note that the symmetry transformation, Eq. (42), can be also presented in an operator form. For a zero-mass particle the Hamiltonian H and the Dirac operator K are

$$H=\alpha\mathbf{p}+\beta U(r)+V(r),\quad K=-\beta(\sigma l+1) \tag{45}$$

(the quantum number κ is the eigenvalue of the operator K). It can be easily seen that in this case we have

$$\gamma_5 H\gamma_5=\alpha\mathbf{p}-\beta U(r)+V(r),\quad \gamma_5 K\gamma_5=-K, \tag{46}$$

which are the same as Eqs. (42).

6. RESULTS OF NUMERICAL CALCULATIONS

Here we report results of our numerical calculations. In Fig. 4 is shown the dependence of the eigenvalues $\varepsilon_{n\kappa}=E_{n\kappa}/M$ on the ratio $\zeta/|\kappa|$ for potential (27) (the solid lines correspond to the lowest states for a given value of κ, $n=1$; the dashed lines are for the first excited states, $n=2$). The energy eigenvalues decrease monotonically with growing Coulomb parameter ζ, and for $\zeta\to|\kappa|$ they have a square-root singularity. The latter is characteristic

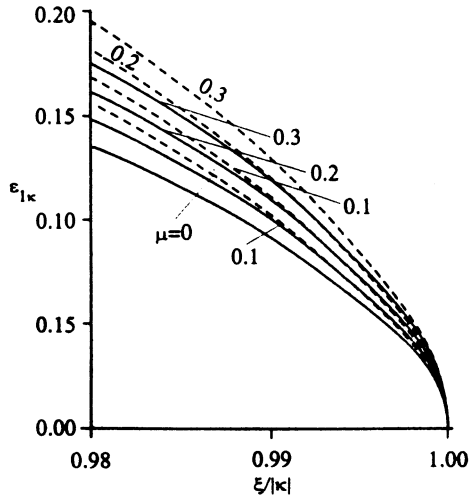

FIG. 5. The eigenvalues $\varepsilon_{1\kappa}(\zeta)$, $n=1$, of the Dirac equation with potential (27) in the vicinity of $\zeta=-\kappa$. The solid curves correspond to the $\kappa=-1$ states, the dotted ones to $\kappa=-2$. The curves are labeled with the values of $\mu=m/M$.

of potentials with a Coulombic behavior at $r\to 0$ and is connected to the phenomenon of the collapse to the center.[10,11]

In Fig. 4 one can see that the levels with $\kappa>0$ lie much higher than those with $\kappa<0$ (for a given n). The physical meaning of this effect becomes clear when one recalls that the centrifugal barrier is proportional to $\kappa(\kappa+1)$ and is absent for $\kappa=-1$ (for example), in contrast to the case of $\kappa=+1$.

Note that the energies of the lowest ($n=1$) states with $\kappa<0$ reach the value $\varepsilon=0$ at the maximal possible value of the Coulomb coupling constant $\zeta=-\kappa$ (Fig. 5). All the other states also have square-root singularities at $\zeta=|\kappa|$, but their energies are positive (Fig. 6). The numerical values of $\varepsilon_{n\kappa}(\zeta)$ in the two extreme cases $\zeta=0$ and $\zeta=|\kappa|$ are given in Table I, where the dependence of $\varepsilon_{n\kappa}$ on the quark

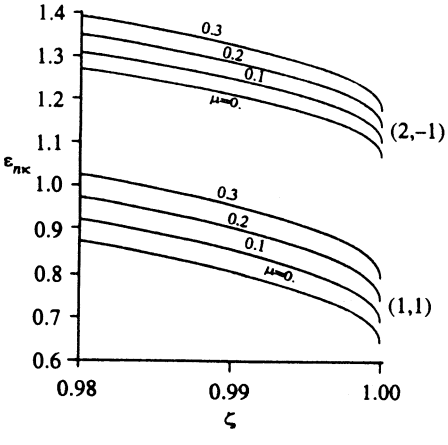

FIG. 6. The same as in the preceding figure, for excited states ($\kappa=-1$, $n=2$ and $\kappa=1$, $n=2$).

mass is also illustrated. Figure 7 shows the energies of several lowest levels within the interval $0.3<\zeta<0.8$, which is of practical interest for the $u\bar{b}$ system[2].

We note that the singularity at $\zeta=|\kappa|$ can be removed when one introduces a cutoff of the Coulomb potential $V(r)=-\zeta/r$ at small distances[3]:

$$V(r)=\begin{cases}-\zeta r^{-1}, & \text{if } r>r_0,\\ (-\zeta/r_0)f(r/r_0), & \text{if } 0<r<r_0,\end{cases} \tag{47}$$

where r_0 is the cutoff radius, and $f(0)<\infty$.

In the case $r_0\ll M^{-1}$ the influence of the cutoff on the energy levels is important only in the immediate vicinity of the point $\zeta=|\kappa|$. Here the level sinks to the boundary $\varepsilon=0$ (it corresponds to a boundary $\varepsilon=-m$ for $m\neq 0$) at some value $\zeta=\zeta_{n\kappa}>|\kappa|$, which depends both on r_0 and on the concrete form of the cutoff function $f(r/r_0)$ in Eq. (47).

With a further increase of ζ the level goes on down to the region of negative values of energy, but the spectrum stays discrete (this is in contrast to the Coulombic problem with a vector potential).[10,11] Thus pair creation does not take place.

7. EXACT SOLUTION FOR $E=0$

In QED the solutions of the Dirac equation simplify considerably for $E=\pm m$, which corresponds in our case ($m=0$) to $E=0$. Equations (28) in terms of linear combinations $u=G+F$, $U=G-F$ assume the form ($\varepsilon=0$)

$$u'-xu+\frac{\kappa+\zeta}{x}v=0,\quad v'+xv+\frac{\kappa-\zeta}{x}u=0. \tag{48}$$

At $\zeta=-\kappa$ the first equation can be solved explicitly:

$$u=C\exp(x^2/2),$$

which yields $C=0$ and hence $G=-F=v/2$. The normalized wave functions are[4]

$$G(x)=-F(x)=\pi^{-1/4}\exp(-x^2/2). \tag{49}$$

Using the perturbation theory in the parameter $(\kappa^2-\zeta^2)^{1/2}\ll 1$, one can determine the behavior of the energy near $\zeta=-\kappa$:

$$\varepsilon(\zeta)=\pi^{-1/2}(1-\zeta^2/\kappa^2)^{1/2}+\ldots \tag{50}$$

(for details see Appendix A). Computations confirm this asymptotic expansion; see Fig. 5.

Note that the solution of the type in (49) exists only for the states with $\kappa<0$. In the case $\zeta=\kappa$, Eqs. (48) have a nonzero solution

$$G=F=\text{const}\cdot\exp(x^2/2)$$

which is not admissible because of the exponential growth at infinity.

These results can be generalized to arbitrary values of ζ and κ. Solving (48) for one of functions u,v, we come to the equation

$$w''+\frac{1}{x}w'-\left[\pm 2+x^2+\frac{\kappa^2-\zeta^2}{x^2}\right]w=0, \tag{51}$$

TABLE I. The eigenvalues $\varepsilon_{n\kappa}$ of the Dirac equation with $\zeta=0$ and $\zeta=|\kappa|$.

		$\zeta=0$		$\zeta=\|\kappa\|$	
n	κ	$\mu=0$	$\mu=0.3$	$\mu=0$	$\mu=0.3$
1	−1	1.61944	1.84441	0.00000	0.00000
2	−1	2.60263	2.80689	1.06901	1.17491
3	−1	3.29118	3.49080	1.96846	2.11712
4	−1	3.85541	4.05300	2.67856	2.84277
1	−2	2.14652	2.36761	0.00000	0.00000
2	−2	2.95197	3.15853	0.64443	0.70949
3	−2	3.57353	3.77508	1.39768	1.51077
4	−2	4.09947	4.29854	2.08531	2.22342
1	−3	2.56927	2.78850	0.00000	0.00000
2	−3	3.26852	3.47647	0.45001	0.49567
1	−4	2.93218	3.15029	0.00000	0.00000
1	1	2.29403	2.49206	0.64015	0.79011
2	1	3.03103	3.22747	1.62588	1.79736
3	1	3.62598	3.82161	2.39019	2.57021
1	2	2.70440	2.90645	0.36916	0.46149
2	2	3.35376	3.55217	1.12003	1.25059
1	3	3.05967	3.26183	0.25449	0.31931
1	4	3.40866	3.60000	0.19328	0.24284

where the upper (lower) sign corresponds to the function $u(v)$. We consider the case $\zeta>|\kappa|$, when the cutoff of the Coulomb part is essential. A solution of these equations for $r>r_0$, decreasing at infinity, can be expressed in terms of Whittaker functions,

$$u=C_1x^{-1}W_{-1/2,ig}(x^2),\quad v=C_2x^{-1}W_{1/2,ig}(x^2),\quad (52)$$

where $g=(\zeta^2-\kappa^2)^{1/2}>0$, and C_1,C_2 are constants.

Insertion of (52) into the first of Eqs. (48) yields the connection between C_1,C_2:

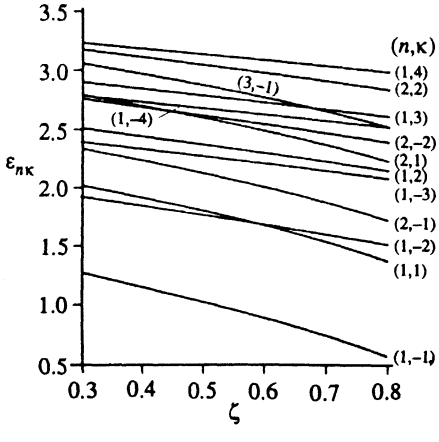

FIG. 7. The energies of the lowest levels, $\varepsilon_{n\kappa}$, versus the Coulomb parameter ζ (for a quark mass $m=0$).

$$C_1=2(\kappa+\zeta)C_2.\quad (53)$$

In the internal region, $0<r<r_0$, the Dirac equation should be solved with cutoff potential (47), where one can neglect the linear potential because of the relation $r_0\ll 1/M$. For the simplest case, $f(x)\equiv 1$ (a square-well cutoff), the solution can be found analytically and can be expressed in terms of Bessel functions with half-integer index.

The energy spectrum is found from the joining of the internal and external solutions at $r=r_0$. In the case of the Dirac equation one can join the ratio F/G instead of the logarithmic derivative.

As a result we have

$$2(\kappa+\zeta)W_{-1/2,ig}(x_0^2)/W_{1/2,ig}(x_0^2)=\xi,\quad (54)$$

where $\xi=u(x_0)/v(x_0)$ is determined from the interval solution and depends on κ,ζ and the cutoff model. For the states with $\kappa=\mp 1$ in the square-well cutoff case, we have

$$\xi|_{\kappa=-1}=-\frac{1}{\xi}\Big|_{\kappa=1}=\frac{1-\zeta(1+\operatorname{ctg}\zeta)}{1+\zeta(1-\operatorname{ctg}\zeta)}.\quad (55)$$

Equation (54) can be solved numerically; it determines the dependence of the Coulomb constant $\zeta_{n\kappa}$, which corresponds to the descent of the n-th level to the boundary $\varepsilon=0$, on the cutoff radius r_0 [for a certain choice of the cutoff function $f(r/r_0)$].

TABLE II. Values of the parameter ρ in Eq. (58).

n	κ	$\zeta=0$		$\zeta=\lvert\kappa\rvert$	
		$\mu=0$	$\mu=0.3$	$\mu=0$	$\mu=0.3$
1	−1	0.15534	0.13156	1.00000	1.00000
2	−1	0.20341	0.17727	0.50983	0.44930
3	−1	0.21280	0.18976	0.35668	0.31909
4	−1	0.21640	0.19580	0.30697	0.27815
1	−2	0.16165	0.14188	1.00000	1.00000
2	−2	0.19556	0.17401	0.66958	0.61953
3	−2	0.20662	0.18651	0.47148	0.43447
4	−2	0.21178	0.19318	0.38478	0.35496
1	−3	0.16444	0.14718	1.00000	1.00000
1	−4	0.16601	0.15049	1.00000	1.00000
1	1	0.22266	0.18839	0.34861	0.31937
1	2	0.20986	0.18360	0.54374	0.51578
1	3	0.20203	0.18024	0.65694	0.63317
1	4	0.20532	0.17791	0.72679	0.70663

Finally, we note that a solution (49) can be generalized to the case of nonzero quark mass and an arbitrary scalar potential $U(r)$. There is an exact solution of the Dirac equation with $\zeta=-\kappa$ and $E=0$,

$$G_0(r)=-F_0(r)=N\exp\left[-\int_0^r m(r')dr'\right], \qquad (56)$$

where $m(r)=m+U(r)$ is a variable quark mass and N is the normalization constant, [see Eq. (A8)]. Since this wave function has no nodes, this solution corresponds to the lowest ($n=1$) level with the fixed κ. The energy of the state, as well as other physical quantities, has a square-root singularity at $\zeta\to-\kappa$, characteristic of the relativistic Coulomb problem:

$$E(\zeta)=c_1\beta+O(\beta^2), \quad \rho=1-c_2\beta+\dots, \qquad (57)$$

where $\beta=(1-\zeta^2/\kappa^2)^{1/2}$, and ρ is the relative weight of the lower component of the Dirac bispinor,

$$\rho=\int_0^\infty F^2(r)dr \Big/ \int_0^\infty G^2(r)dr. \qquad (58)$$

It can be shown that

$$c_1=N^2, \quad c_2=4N^2\langle r\rangle \qquad (59)$$

(see Appendix A), where $\langle r\rangle$ is the mean radius of the bound state (56). The effective-potential method given in Appendix A is most useful in deriving these formulas, as well as for a quantitative analysis of the wave functions near $\zeta=\pm\kappa$.

As is seen from Eq. (57), at $\zeta\approx|\kappa|$ the parameter ρ is close to one (see also Table II). This means that the motion of a light quark is definitely relativistic. The coefficients c_1 and c_2 for a particular case of $m(r)=m+\sigma r$ are presented in Fig. 8. Finally, let us note that square-root singularities of the type of (57) are directly connected with the behavior of the Coulomb potential at $r\to0$ and disappear when it is regularized at small distances.

8. DISCUSSION AND CONCLUSION

In conclusion we discuss the structure of the resulting spectrum, briefly compare it to experiment, and summarize our results[5].

We start with the nonrelativistic spectrum and use the formulas given in Appendix B, which yield the spectrum shown in Fig. 9a. Here the splitting between the $S=1$ and $S=0$ ($L=0$) levels is due to the hyperfine interaction and,

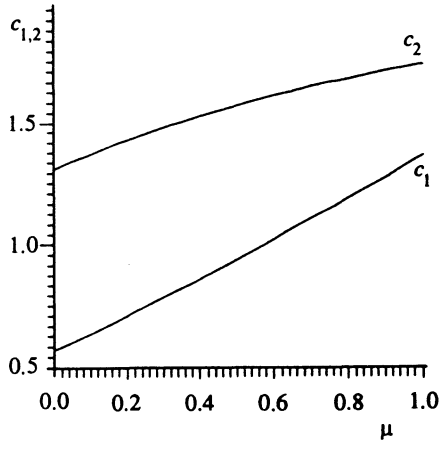

FIG. 8. Dependence of c_1 and c_2 [Eq. (59)] on the quark mass.

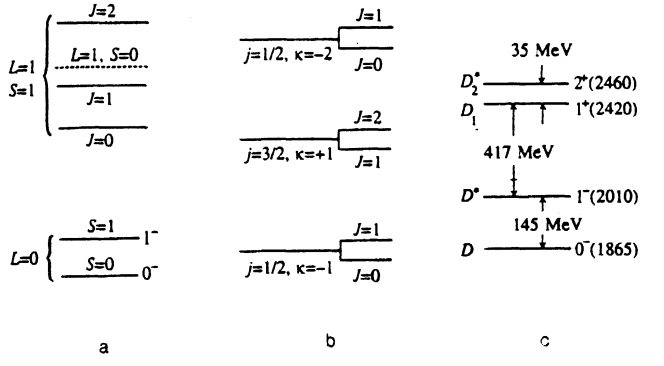

FIG. 9. Energy spectrum for the heavy quark-light antiquark system (qualitative). a—$m_1, m_2 \gg M = \sigma^{1/2}$; b—$m_1 \to 0, m_2 \to \infty$; c—experiment. The energy scale in part a is much larger then in parts b and c.

as is seen in Appendix B, is proportional to $(m_1 m_2)^{-1}$. When both masses are large ($m_i \gg M = \sigma^{1/2}$), all splittings are small, including the spin-spin $[O((m_1 m_2)^{-1})]$ and spin-orbit splittings, which contains terms $O(m_1^{-2})$, $O(m_2^{-2})$ and $O[(m_1 m_2)^{-1}]$, which one can denote as $(LS)_1$, $(LS)_2$ and $(LS)_{12}$—see Appendix B.

In the case $m_2 \gg m_1 \sim M$ (Fig. 9b), the intervals of $(LS)_1$ become the largest, and the spectrum transforms in such a way that the coupling of the spin of particle 2 becomes very weak. In the limit $m_2 \to \infty$ it finally decouples, leading to the Isgur-Wise symmetry.[5] Namely, the states can be classified by the total momentum of the light particle j, while the states of total momentum of the system $J = j + S_2$ are degenerate with respect to the direction of S_2.

This is what one observes in the Dirac spectrum (see Fig. 4 of our numerical calculations and Fig. 9b, which give a schematic description of the Dirac spectrum). Here the degeneracy (Isgur–Wise symmetry) is complete.

This should be compared to the experimental picture in Fig. 9c, where for the charmed mesons the order of the levels is the same as in Fig. 9b, but the splittings are still large. For B-mesons the splitting of lowest levels is smaller by a factor of 3 (52 MeV), as it should be, since the mass of the c quark is ≈ 3 times smaller than that of b quark. We also note that the experimental splitting $\Delta E \sim 450$ MeV between $j = 1/2$ and $j = 3/2$ states is reproducible in our results when one takes $\sqrt{\sigma} \sim 0.5$ GeV and $\zeta \sim 0.6 \div 0.8$.

Thus we can conclude that the Dirac equation yields a reasonable qualitative description of the actual spectrum. We hope to discuss this point in more detail in future publications, where we will also give predictions for the D_S-, B-, and B_S-mesons.

Summarizing our results, we have derived the Dirac equation from the Feynman-Schwinger representation of the quark-antiquark Green's function in case of the color Coulomb interaction.

Assuming that the confining interaction can be introduced into the Dirac equation in the sameway as to the Coulomb interaction, we have clarified the Lorentz structure of the confining interaction connecting a light quark to a heavy antiquark.

The analysis of the solutions of the Dirac equation shows that a potential growing at infinity yields confinement only if it is a scalar, not the time component of a 4-vector. In this aspect there is an essential difference from the nonrelativistic case.

We have also studied the dependence of the charge ζ in the critical region, $\zeta \sim |\kappa|$, and found its dependence on the cutoff of the Coulomb potential. We have computed energy eigenvalues for several lowest levels and have compared them with the nonrelativistic spectrum and experimental results.

After this paper had been finished and submitted for publication, we learned of several papers[28–30] in which analogous problems are discussed[6].

In the paper by Ono,[29] a relativistic generalization of the Richardson potential was considered. The Coulomb part of the potential was considered as a 4-vector component, and its confining part as a relativistic scalar. The paper by Dremin and Leonidov[30] discusses the properties of solutions of the Dirac equation with scalar and vector coupling. Using the squared Dirac equation, the authors arrived at the conclusion that it is only in the case of a scalar potential growing at infinity that bound states can exist in the system. That conclusion is in full agreement with the results of our Sec. 4, where we study in greater detail the asymptotics of the Dirac wave functions at infinity and give a physical explanation of the above results using the effective potential method.

APPENDIX A

Method of effective potential

The system of Eqs. (25) can be reduced to an equivalent Schrödinger equation with a potential depending on energy and having, in general, a rather complicated form[7]. There is a considerable simplification if $\zeta = |\kappa| = 1, 2, \ldots$. This case we shall discuss further.

First let $\zeta = -\kappa$. Proceeding in Eqs. (27) to the linear combinations $u = G + F$, $v = G + F$, we obtain equations from which the function v is easily excluded. Then we get

$$u'' + [\varepsilon^2 - 1 - (x+\mu)^2 + 2\zeta\varepsilon x^{-1}]u = 0, \quad u(0) = 0,$$
$$\int_0^\infty \left(1 + \frac{\zeta}{\varepsilon x}\right) u^2(x)\,dx = \frac{1}{4}, \tag{A1}$$

i.e., the Schrödinger equation with the effective energy $\tilde{E}$ and potential $\tilde{U}$

$$\tilde{E} = \frac{1}{2}(\varepsilon^2 - 1), \quad \tilde{U} = \frac{1}{2}(x+\mu)^2 - \varepsilon\zeta x^{-1}. \tag{A2}$$

Note that the boundary condition at zero for $u(x)$ follows from the fact that we have $A/B = -1$ in Eq. (29), and the normalization condition in (A1) corresponds to the usual condition

$$\int_0^\infty (G^2+F^2)dr=1$$

for the discrete spectrum.

In particular, for $\varepsilon=0$ we have $\tilde{E}=-1/2$, which cannot be an eigenvalue for the harmonic oscillator. Therefore, we have $u(x)\equiv 0$ and $v'+(x+\mu)v=0$, from which the exact solution (49) follows.

For the case $\zeta=\kappa$ the function v, but not u, satisfies an equation of the like (A1), and we have $\tilde{E}=(\varepsilon^2+1)/2$. Here we have $\tilde{E}=1/2$ with $\varepsilon=0$; therefore we have $v(x)\equiv 0$ (with the boundary condition at zero taken into account), while all nonzero solutions $u(x)$ increase exponentially at infinity. Thus, the Dirac equation has no physically acceptable solutions with zero energy if $\zeta=\kappa>0$.

The following results are obtained from (A2). Let $E_n=E_n(\alpha,\mu)$ be the energy spectrum of the Schrödinger equation with the potential

$$V(r)=\frac{1}{2}(r+\mu)^2-\alpha r^{-1}, \tag{A3}$$

with $0<r<\infty$ and $l=0$ [in particular, $E_n(0,0)=2(n-1/4)$, $n=1,2,3,...$]. Then the eigenvalues $\varepsilon_n^{(\mp)}$ of the problem considered may be obtained from the transcendental equation:

$$E_n(|\kappa|\varepsilon,\mu)=\frac{1}{2}(\varepsilon^2\pm\operatorname{sgn}\kappa) \tag{A4}$$

(the $\pm$ sign coincides with the sign of the quantum number κ). Due to the relations

$$\frac{\partial E_n}{\partial\alpha}=-\left\langle\frac{1}{r}\right\rangle,\quad \frac{\partial E_n}{\partial\mu}=\langle r\rangle+\mu,$$

sometimes called the Hellmann-Feynman theorem, the energies $E_n(\alpha,\mu)$ decrease monotonously as the Coulomb parameter α goes up and increase with the growing μ. Taking this into account, we get

$$\varepsilon_1^{(-)}=0<\varepsilon_1^{(+)}<\varepsilon_2^{(-)}<\varepsilon_2^{(+)}<... \tag{A5}$$

(with fixed $|\kappa|$). The results of the numerical solution are given in Table I.

The results are easily generalized to the case of an arbitrary scalar potential $U(r)$. Instead of (A1) we get

$$\frac{d^2\chi}{dr^2}+\left\{E^2-[m+U(r)]^2+(\operatorname{sgn}\kappa)\frac{dU}{dr}+\frac{2|\kappa|E}{r}\right\}\chi=0, \tag{A6}$$

where $\chi(0)=0$, and the normalization condition does not depend explicitly on the form of $U(r)$:

$$\int_0^\infty\left(1+\frac{|\kappa|}{Er}\right)\chi^2(r)dr=\frac{1}{4} \tag{A7}$$

[$\chi=u(r)$ for the states with $\zeta=-\kappa$ and $\chi=v(r)$ for those with $\zeta=\kappa$].

At $\zeta=-\kappa$ there is an exact solution of the Dirac equation which corresponds to zero energy [and does not depend explicitly on κ; see Eqs. (54)]; here $\chi_0(r)\equiv 0$,

$$G_0(r)=-F_0(r)=N\exp\left[-\int_0^r m(r')dr'\right],$$

$$N=\left\{2\int_0^\infty dr\exp\left[-2\int_0^r m(r')dr'\right]\right\}^{-1/2}. \tag{A8}$$

The behavior of the energy of the state at $\zeta\to-\kappa$ can be also determined. Assuming

$$E=c_1\beta+O(\beta^2),\quad \beta=(1-\zeta^2/\kappa^2)^{1/2}\to 0,$$

$$u=\beta u_1(r)+...,\quad v=v_0+\beta v_1(r)+..., \tag{A9}$$

and substituting these expansions into (25), we obtain

$$\frac{du_1}{dr}-mu_1+c_1v_0=0,\quad \frac{dv_1}{dr}+mv_1=\frac{2|\kappa|}{r}u_1. \tag{A10}$$

The solution of the first equation which decreases at infinity has the form

$$u_1(r)=2c_1N\exp\left[\int_0^r m(r')dr'\right]\int_r^\infty dx\times\exp\left[-2\int_0^x m(x')dx'\right], \tag{A11}$$

while the function $v_1(r)$ is calculated by a quadrature; at $r=0$ we have $u_1(0)=c_1/N$, $v_0(0)=2N$. Let

$$\xi(r)\equiv u/v=\beta u_1/v_0+O(\beta^2);$$

then it follows from Eq. (28) that

$$\xi(0)=\frac{A+B}{A-B}=\frac{(1+\beta)^{1/2}-(1-\beta)^{1/2}}{(1+\beta)^{1/2}+(1-\beta)1/2}=\frac{1}{2}\beta+O(\beta^2)$$

whence $u_1/v_0|_{r=0}=1/2$, and finally we get Eq. (59) for c_1.

Thus for the states whose energy vanishes at $\zeta=-\kappa$, the coefficient of the square-root singularity in $E(\zeta)$ can be found explicitly for an arbitrary scalar potential $U(r)$. Other physical quantities, such as ρ, have the same singularities at $\zeta=-\kappa$.

Using Eqs. (25) and (A6), we find for the parameter ρ introduced in (58) that

$$\rho=\frac{1-s}{1+s},\quad s=2\int_0^\infty uvdr\Big/\int_0^\infty(u^2+v^2)dr$$

$$=\int_0^\infty m(r)\chi^2dr\Big/\int_0^\infty\left(E+\frac{|\kappa|}{r}\right)\chi^2dr$$

$$=\frac{4}{E}\int_0^\infty m(r)\chi^2dr \tag{A12}$$

[here $\zeta=|\kappa|$, and in the latter formula $\chi(r)$ is normalized according to Eq. (A7)]. Hence, expansion (57) for ρ follows, where

$$c_2=2\int_0^\infty u_1v_0dr.$$

Substituting in the above expressions for u_1,v_0, and changing the order of integration, we obtain

$$c_2=8c_1^2\int_0^\infty\exp\left[-2\int_0^r m(r')dr'\right]rdr, \tag{A13}$$

which coincides with Eq. (59).

Let us consider a few simple dependences $m(r)$.

1) A constant mass $m(r)=m$ corresponds to QED. At $\zeta=-\kappa$, we have

$$G_0=-F_0=m^{1/2}e^{-mr},\quad c_1=m,\quad c_2=2, \tag{A14}$$

which corresponds to the Sommerfeld formula for the relativistic Coulomb problem, which has the following form for the $\kappa=-n$ states ($j=l+1/2=n-1/2$):

$$E_{nj}(\zeta)=m\left(1-\frac{\zeta^2}{n^2}\right)^{1/2}\equiv m\beta,\quad \rho=\frac{1-\beta}{1+\beta}. \tag{A15}$$

The levels with radial quantum numbers $n_r>0$ also have the Coulomb singularity at $\zeta\to|\kappa|$, but the corresponding energies are positive. For example, for the $ns_{1/2}$ states ($k=-1$, $n_r=n-1$):

$$E_{n,1/2}=m\left(\frac{n-1}{N}+\frac{\beta}{N^3}+\ldots\right),$$

$$\rho_n=(N+n-1)^{-2}\left(1-\frac{2n}{N}\beta+\ldots\right), \tag{A16}$$

where $\beta=(1-\zeta^2)^{1/2}$, $\zeta=Z\alpha\to 1$, and $N=(n^2-2n+2)^{1/2}$.

At $n\gg 1$ we find $\rho_n=1/4n^2\to 0$, and the bound states become nonrelativistic.

2) At $m(r)=m+\sigma r$, we find

$$G_0=-F_0=N\exp\{-(\sigma r^2/2+mr)\}, \tag{A17}$$

$$N=(\sigma/\pi)^{1/4}[\exp(\mu^2)\cdot\operatorname{erf}c(\mu)]^{-1/2},\quad \mu=m/\sigma^{1/2},$$

$$c_1=N^2,\quad c_2=4\sigma^{-1}c_1(c_1-m) \tag{A18}$$

(note that the dimensionless coefficient c_2 depends only on μ). In the extreme case at $\mu\ll 1$ we obtain

$$c_1=\left(\frac{\sigma}{\pi}\right)^{1/2}\left(1+\frac{2\mu}{\pi^{1/2}}+\ldots\right),\quad c_2=\frac{4}{\pi}\left(1+\frac{4-\pi}{\pi^{1/2}}\mu+\ldots\right), \tag{A19}$$

while at $\mu\gg 1$ we obtain

$$c_1=m\left(1+\frac{1}{2}\mu^{-2}+\ldots\right),\quad c_2=2-\mu^{-2}+\ldots \tag{A20}$$

Numerical results for c_1, c_2 are given in Fig. 9.

APPENDIX B

The nonrelativistic spectrum of two particles with all spin interactions taken into account can be obtained in the perturbative way ($1/m$ expansion):

$$m=m_1+m_2+E(n)+\left\langle n\left|\left(\frac{\sigma_1\mathbf{L}}{m_1^2}+\frac{\sigma_2\mathbf{L}}{m_2^2}\right)\left(\frac{1}{4r}\frac{d\varepsilon}{dr}\right.\right.\right.$$

$$\left.+\frac{1}{2r}\frac{dV_1}{dr}\right)+\frac{(\sigma_1+\sigma_2)\mathbf{L}}{2m_1m_2}\frac{1}{r}\frac{dV_2}{dr}+\frac{\sigma_1\sigma_2}{12m_1m_2}V_4(r)$$

$$\left.\left.+\frac{1}{12m_1m_2}(3\sigma_1 n\cdot\sigma_2 n-\sigma_1\sigma_2)V_3(r)\right|n\right\rangle. \tag{B1}$$

The contributions of the scalar interaction $U(r)=\sigma r$ and the vector interaction $V(r)=-4\alpha_s/3r$ to the spin splittings are

$$\frac{1}{r}\frac{d\varepsilon}{dr}=\frac{\sigma}{r}+\frac{4}{3}\frac{\alpha_s}{r^3},\quad \frac{1}{r}V_1'=-\frac{\sigma}{r},\quad \frac{1}{r}V_2'=\frac{4}{3}\frac{\alpha_s}{r^3},$$

$$V_4=\frac{32\pi\alpha_s}{3}\delta^{(3)}(r),\quad V_3=\frac{4\alpha_s}{r^3}. \tag{B2}$$

The main difference appears in V_1', where only the scalar interaction enters. Note that the overall signs of the spin-orbit terms due to the scalar (σr) and vector ($-4\alpha_s/3r$) potentials are different.

[1)] Thanks are due to D. Popov for the derivation of the relations and for verification of Eqs. (29)–(31).

[2)] As can be seen from Figs. 5 and 6, the dependence of the energy $\varepsilon_{n\kappa}$ on the light-quark mass is practically linear. This is in agreement with Ref. 27, where the energy spectrum of Eq. (25) was calculated at $\zeta=0.6$ with hyperfine splitting taken into account, which is necessary for a detailed comparison with the experimental spectrum (the procedure was similar to the calculation of the hyperfine structure for relativistic Coulomb problem). The value of hyperfine splitting obtained in Ref. 27 differs from experimental data for charmonium and bottomonium by over 30%.

[3)] In the case of the lowest levels with $\kappa<0$, for which $\varepsilon(\kappa)\to 0$ in the limit $\zeta\to|\kappa|$ (see Fig. 4), this singularity can be derived analytically—see Eq. (50) below.

[4)] This result can be easily generalized to the case $m\neq 0$ and arbitrary scalar potential $U(r)$.

[5)] The main results of this paper were presented in Ref. 8.

[6)] The authors are indebted to A. E. Kudryavtsev who pointed out to us the above mentioned papers.

[7)] See Refs. [10,24,26] on physical phenomena near the boundary of the lower continuum $E=-mc^2$ in QED,[10] where the above method was successfully applied.

[1] B. Grinstein, Preprint HUTP-91/A028 (1991). J. D. Bjorken, Preprint SLAC-PUB-5278.

[2] Yu. A. Simonov, Nucl. Phys. B **324**, 67 (1989). M. Schiestl and H. G. Dosch, Phys. Lett. B **209**, 85 (1988).

[3] D. Gromes, Preprint HD-THEP-87-21 (1987).

[4] W. Lucha, F. Schöberl, and D. Gromes, Phys. Rep. **200**, 127 (1991).

[5] M. Isgur and M. Wise, Phys. Lett. B **232**, 113 (1989); **327**, 527 (1990).

[6] H. G. Dosch and Yu. A. Simonov, Phys. Lett. B **205**, 339 (1988). H. G. Dosch, Phys. Lett. B **190**, 177 (1987).

[7] Yu. A. Simonov, Nucl. Phys. B **307**, 512 (1988); Yad. Fiz. **54**, 192 (1991) [Sov. J. Nucl. Phys. **54**, 115 (1991)].

[8] V. D. Mur, V. S. Popov, Yu. A. Simonov, and V. P. Yurov, Preprint ITEP 83-92 (1992).

[9] I. Pomeranchuk and Ya. Smorodinsky, J. of Phys. USSR **9**, 315 (1945).

[10] Ya. B. Zel'dovich and V. S. Popov, Uspekhi Fiz. Nauk **105**, 403 (1971) [Usp. Fiz. Nauk **14**, 673 (1971)].

[11] W. Greiner, B. Müller, and J. Rafelski, *Quantum Electrodynamics of Strong Fields*, Springer-Verlag, Heidelberg (1985).

[12] A. M. Polyakov, Nucl. Phys. B **164**, 171 (1980). V. S. Dotsenko and S. N. Vergeles, Nucl. Phys. B **169**, 527 (1980). R. A. Brandt, A. Gocksch, M.-A. Sato, and F. Neri, Phys. Rev. D **26**, 3611 (1982).

[13] Yu. A. Simonov and J. A. Tjon, Ann. Phys. (N.Y.) (1993) (in press).

[14] V. Marquard and H. G. Dosch, Phys. Rev. D **35**, 2238 (1987).

[15] M. Shifman, A. Vainshtein, and V. Zakharov, Nucl. Phys. B **147**, 385, 448 (1979).

[16] M. Campostrini, A. Di Giacomo and G. Mussardo, Z. Phys. C **25**, 173 (1984). A. Di Giacomo and H. Panagopoulos, Phys. Lett. B **285**, 133 (1992).

[17] Yu. A. Simonov, Z. Phys. C **53**, 419 (1992).

[18] Yu. A. Simonov, Phys. Lett. B **226**, 151 (1989).

[19] W. Buchmüller, Phys. Lett. B **112**, 479 (1982). R. D. Pisarski and J. D. Stack, Preprint Fermilab PUB-86/122-T (1986).

[20] A. I. Akhiezer and V. B. Berestetsky, *Quantum Electrodynamics*, Nauka, Moscow (1969) (in Russian).
[21] L. D. Landau and E. M. Lifshitz, *Quantum Mechanics*, Pergamon, New York (1991).
[22] K. M. Case, Phys. Rev. **80**, 797 (1950).
[23] W. Pieper and W. Greiner, Z. Phys. **218**, 327 (1969).
[24] V. S. Popov, Pis'ma v ZhETF **11**, 254 (1970) [JETP Lett. **11**, 162 (1970)]; Yad. Fiz. **12**, 429 (1970) [Sov. J. Nucl. Phys. **12**, 235 (1971)].
[25] V. D. Mur and V. S. Popov, Yad. Fiz. **18**, 684 (1973).
[26] V. S. Popov, Yad. Fiz. **14**, 458 (1971).
[27] D. Pignon and C. A. Piketty, Phys. Lett. B **81**, 334 (1979).
[28] F. Ravndal, Phys. Lett. B **113**, 57 (1982).
[29] S. Ono, Phys. Rev. D **26**, 2510 (1982).
[30] I. M. Dremin, A. V. Leonidov, Pis'ma v ZhETF **37**, 617 (1983) [JETP Lett. **37**, 738 (1983)].

Translated by the authors

Edited by D. Parsons